Journal of Applied Electrochemistry **34**: 1103–1112, 2004.

In situ analysis of high temperature characteristics of prismatic polymer lithium - ion batteries

MOHAMED MOHAMEDI[1,2]*, HIROAKI ISHIKAWA[1] and ISAMU UCHIDA[1]
[1]*Department of Applied Chemistry, Graduate School of Engineering, Tohoku University, 07 Aramaki Aoba, Aoba-Ku, Sendai 980-8579, Japan*
[2]*Present address: Advanced Research Institute for Science and Engineering, Waseda University, Shillman, Hall#702, Shinjuku-ku, Okubo 3-4-19, Tokyo 169-8555, Japan*
*(*author for correspondence, e-mail: mohamed@kurenai.waseda.jp)*

Received 3 June 2003; accepted in revised form 4 June 2004

Key words: ac impedance, kinetic parameters, polymer lithium-ion battery, safety, state-of-charge, thermal characteristics

Abstract

A systematic approach to understanding the safety fundamentals of Li-ion batteries was undertaken. Firstly, we present thermal characterization experiments of charged prismatic polymer lithium-ion batteries (PLBs). These cells, at different state of charge (SOC), were tested inside an accelerated rate calorimeter (ARC) to determine the onset-of-thermal runaway (OTR) temperatures. In addition, the thermally activated components of these cells were followed by monitoring both the impedance (at 1 kHz) and the open circuit voltage (OCV) as a function of temperature. An increase in the impedance was observed at around 133 °C corresponding to the polyethylene separator shutdown. Secondly, an original *in situ* ac impedance measurement was performed over a wide range of frequencies instead of 1 kHz when the battery was heated from ambient to 130 °C. Resulting impedance spectra were modeled using an appropriate equivalent circuit. It is concluded that the high frequency and the low frequency semicircles observed in the impedance spectra are due to processes occurring the anode/electrolyte and cathode/electrolyte interfaces, respectively. The activation energy E_a was found in the ranges of 0.4–0.6 and 0.36–0.53 eV, for cathode and anode processes, respectively. In addition, it is assumed that change in the electrolyte composition is the main factor responsible for the rise in the cell impedance at high temperatures.

1. Introduction

Safety is a general challenge for Li-ion batteries, and an increasing amount of research now focuses on this aspect. During battery charge/discharge, various chemical and electrochemical reactions as well as transport processes take place. At elevated temperatures, reactions involving the active electrode material, electrode binder, and the non-aqueous electrolyte lead to self-heating of the cell thereby causing the cell temperature to rise without further external heating. This condition, usually referred to as the thermal runaway condition, could potentially lead to catastrophic disassembly of the cell [1–3]. Therefore, quantitative measurements of the heat generation rate inside the battery during normal and abuse conditions are important to design and develop a suitable thermal management system for scaled-up battery systems. Such measurements can be obtained using the accelerated rate calorimeter (ARC). Safety features provided by the thermally activated components in several-charged or discharged Li-ion cells can be studied by monitoring the impedance (internal resistance) and the open circuit voltage (OCV) of these cells as a function of temperature [3, 4].

In the first section of this paper, we report on characterization of thermal cut-off for charged prismatic polymer lithium-ion batteries (PLBs), i.e., the thermally activated components of the cells were followed by monitoring the impedance (at 1 kHz) and the OCV as a function of temperature.

In the second section, we describe an original method, which consisted in recording *in situ* ac impedance behavior over a wide range of frequencies when the battery was heated from ambient to 130 °C. The objective of this second section is twofold: (i) in combination with thermal runaway measurements, to attempt to identify factors responsible for the rise in cell impedance at high temperatures, and (ii) evaluation of kinetic parameters of the polymer Li-ion cell reaction.

Such a systematic study on the high temperature dependence of ac impedance behavior of polymer Li-ion batteries has not been reported.

2. Experimental details

2.1. *Cell specifications*

Commercial sealed prismatic polymer lithium-ion cells of 3 mm in thickness, 33 mm in width and 48 mm in length were used. The cells had a $LiCoO_2$-based cathode, a MCMB-based anode, PVDF-PC-EC-$LiPF_6$ polymer electrolyte, and a polyethylene (PE) separator. The nominal capacity of the cell, as rated by the manufacturer, was 0.5 Ah at ambient temperature.

2.2. *Thermal cut-off measurements*

Experiments were carried out inside an accelerated rate calorimeter (ARC) 2000™ (Columbia Scientific Industries) in combination with a battery cycler (TOSCAT-5000U, Toyo System Co.). The current, voltage and thermocouple outputs from the test cells were connected to monitoring equipment outside the ARC.

The cell was placed inside the ARC cavity, was first charged to the desired SOC, and was left at OCV condition for at least 12 h. Then the cell was heated stepwise to thermal runaway conditions. The cell temperature was measured with a thermocouple attached to the cell surface. The experimental sequence is based on the ARC heat-wait search (HWS) mode, where the cell temperature is increased 10 °C min^{-1} in each step followed by 30 min wait time. During wait time, if the self-heating rate of the cell is larger than 0.05 °C min^{-1}, this is considered an indication of the onset of an exothermic reaction. The ARC then shuts down the heating and records the cell temperature up to the end of the thermal runaway process. The internal impedance of the cells was measured at 1 kHz using a Hewlett-Packard 4338B Milliohmmeter and OCV was measured using a Keithley 610C.

2.3. In situ *ac impedance measurements*

Electrochemical impedance spectroscopy (EIS) measurements at several SOC values were performed inside the ARC (Figure 1). The cell was placed inside the ARC cavity and was first charged to the required SOC, and allowed to stand for at least 12 h under OCV conditions prior to the measurements. Then, the cell was heated stepwise (10 °C min^{-1}) from 25 to 130 °C following the experimental sequences shown in Figure 2. At the desired temperature, 1 h wait time was allowed before recording impedance spectra. Impedance measurements were carried out using a Solartron 1286/1260 system that covered the frequency range from 10 kHz to 100 mHz with an ac voltage of 10 mV.

2.4. *Impedance data analysis procedure*

The impedance data of sealed commercial cells are rather tedious to analyze since the results are generally

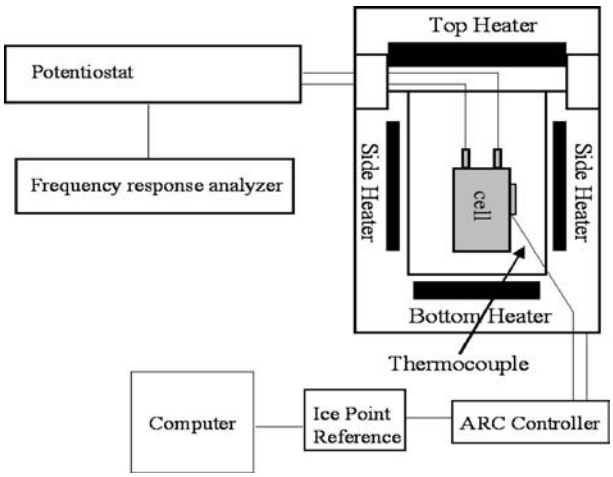

Fig. 1. Experimental accelerated rate calorimeter (ARC) for studying thermal cut-off characteristics of Li-ion cells.

the superposition of several processes taking place at both the positive and the negative electrodes. A direct estimation of the individual electrode parameters is not possible since a suitable reference electrode cannot be introduced into a commercial sealed cell. Nevertheless, systematic linear and reproducible variations of measurable or computable impedance parameters with battery conditions are useful indications of the SOC in a non-destructive way. Thus, impedance data were modeled by means of an equivalent circuit, and the fitting procedure evaluated with a complex non-linear least squares (CNLLS) 'EQUIVCRT' program developed by Boukamp [5]. The impedance parameters, which exhibit a dependence on SOC and temperature, are used for evaluation of kinetic parameters of the PLB reaction.

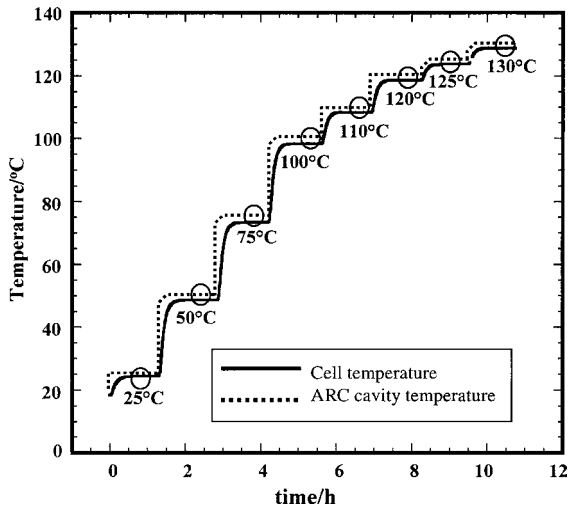

Fig. 2. Experimental protocol followed during recording *in situ* impedance spectra over a wide range of frequencies. The cells charged to several SOCs were heated from ambient to 130 °C. Circles indicate where impedance measurements were performed.

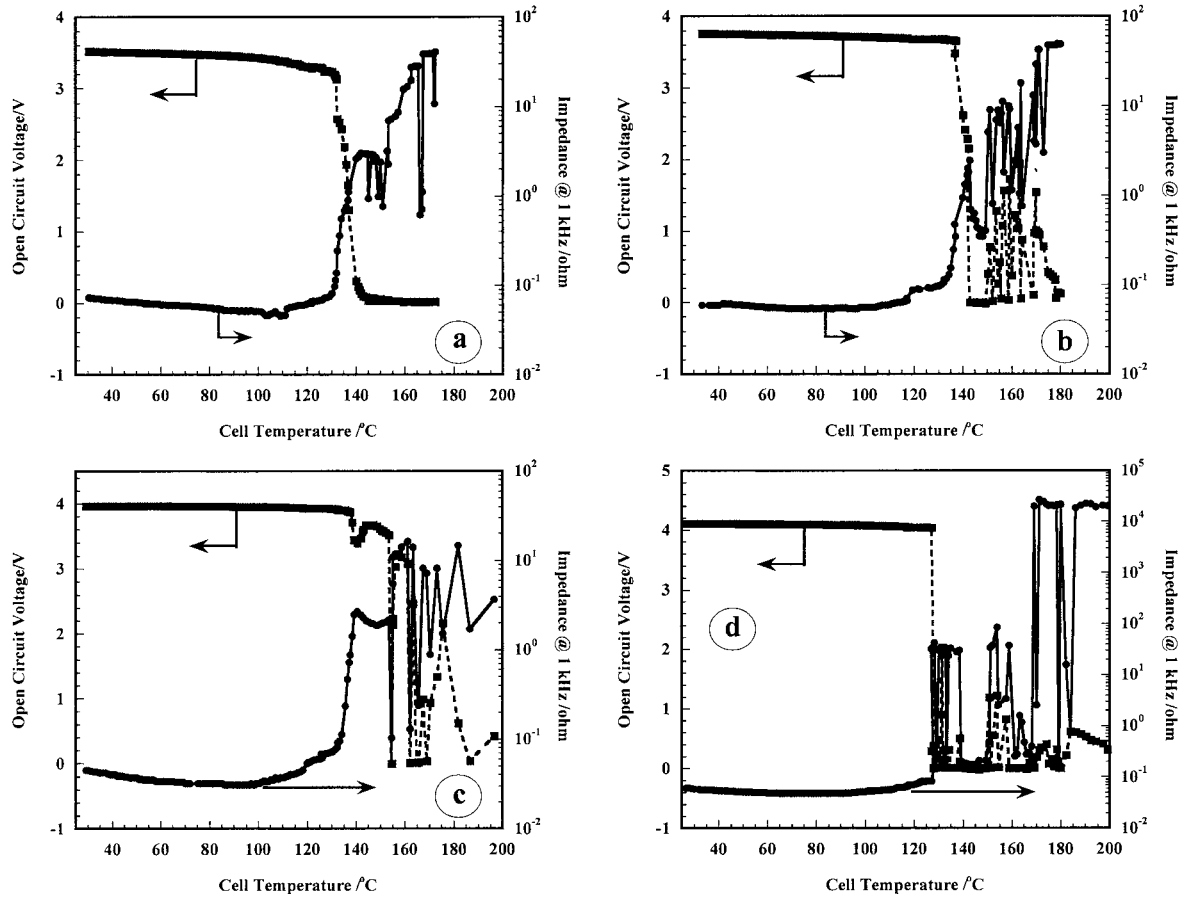

Fig. 3. Internal impedance at 1 kHz and open-circuit voltage (OCV) as function of temperature for Li-ion cells charged to (a) 0, (b) 25, (c) 75, and (d) 100% SOC.

3. Results and discussion

3.1. *The ARC measurements of thermal run-away*

Figure 3 shows impedance (at 1 kHz) and open-circuit voltage (OCV) as a function of temperature for cells charged to several SOCs. Increasing cell temperature resulted in an increase in the impedance value (by ca. 2–3 orders of magnitude) at around 133 °C for all cells. The increase in impedance at around 133 °C is due to the polyethylene separator shutdown mechanism in the microporous separator membrane present in the Li-ion cells [6–8].

PE separators are used as secondary safety mechanisms, which help to limit cell temperatures by melting. The separator is microporous and, at the melting point, the pores collapse to the form of a relatively non-porous insulating film between the anode and the cathode [9]. Consequently, ion transport between the anode and cathode drastically decreases, thereby leading to an increase in cell impedance and passage of current through the cell is restricted [4, 9]. This prevents further electrochemical activity in the cell, thereby shutting the cell down before an explosion occurs. At the same time, the cell cannot experience a short through pinholes formed in the separator for the OCV to become zero. If shorting takes place, the impedance should also decrease. An appropriate explanation may be as follows; when pores of the separator are closed, there is electrical isolation of the electrodes due to inaccessibility of the electrolyte through the separator. This can cause the OCV to fluctuate at zero as seen in Figure 3. Furthermore, the electrolyte is converted to vapour state. This can also bring about electrical isolation. Indeed, a post-mortem observation of the cells revealed that they expanded significantly and ruptured irrespective of the SOC. These results indicate that the battery expansion is mainly due to the evolution of non-condensable gases, followed by volumetric expansion of these gases at higher temperature.

3.2. In situ *ac impedance measurements*

It should be understood that when the separator melts as a result of the temperature exceeding its melting point (~125 °C for polyethylene), this frequently triggers a large heat output induced by internal shorting, and thus a significant increase in the internal resistance is observed. In the following we were interested in the cell behavior prior to the separator shutdown temperature.

A careful examination of Figure 3 shows that before reaching the shutdown temperature (~133 °C), the cell

impedance first undergoes a step upward just above 100 °C, which might be considered as the first trigger temperature. Hardly any explanations as to the causes yielding the rise in the cell impedance at high temperatures are reported in the literature. The first trigger temperature has been explained as due to the positive-temperature-coefficient (PTC) that is responsible for the impedance jump taking place at around 110 °C in the impedance-temperature curve [4]. However, cells used in our study did not have any internal or external PTC.

Other causes such as temperature-induced changes in the electrolyte composition or changes in the active electrode materials are also likely to be important. Thus, the question is, 'what is the origin of the increase in impedance possibilities are that?' it comes from the charge-transfer resistance or the resistance of the solid-electrolyte interphase (SEI), or the diffusional impedance inside the cathode matrix (diffusion of Li^+ inside the cathode lattice), or from the ohmic resistance of the cell. Accordingly, *in situ* impedance measurements were performed over a wide range of frequencies following the experimental sequences shown in Figure 2. Representative Nyquist spectra taken at 25 and 120 °C for various SOCs are shown in Figure 4. The spectra are characterized as follows:

(i) The cell impedance in the complex plane is a pair of capacitive semicircles of unequal dimensions. The appearance of these two semicircles depended on temperature, i.e., the high frequency semicircle progressively vanished with increasing temperature. (ii) A Diffusional behavior in the low frequency region. Actually, the diffusion appeared from 50 °C irrespective of the SOC.

The impedance spectrum of a sealed lithium-ion battery reflects the electrochemical processes at the interfaces of both the anode and the cathode. Although extensive efforts were made in recent years, it is quite problematic to determine which semicircle in the impedance spectrum corresponds to each electrode (anode and cathode) because both electrodes play a part in the battery impedance and the kinetics of both electrode reactions are probably similar in magnitude [10]. Similarly to the data of Figure 4, a pair of capacitive semicircles of unequal dimensions has been reported for Li-ions cells [11–14]. The larger semicircle has been attributed to charge-transfer at the carbon anode and the high frequency smaller semicircle to charge transfer at the cathode [11]. However, impedance spectra of the $LiCoO_2$ electrode alone resulted in two semicircles with the high frequency one reflecting the formation of a surface layer (passive film) on the $LiCoO_2$ [15]. Other research on sealed batteries concluded that the

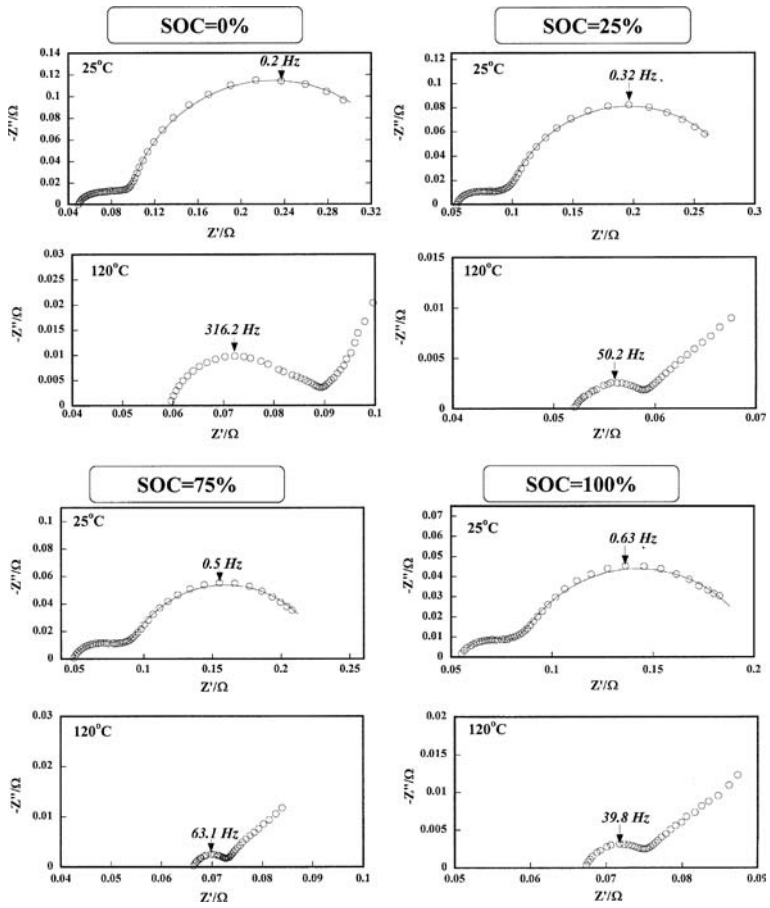

Fig. 4. Representative *in situ* ac impedance spectra at 25 and 120 °C for Li-ion cells charged to several state-of-charges (SOCs are indicated in the figure) following the experimental sequences shown in Figure 2.

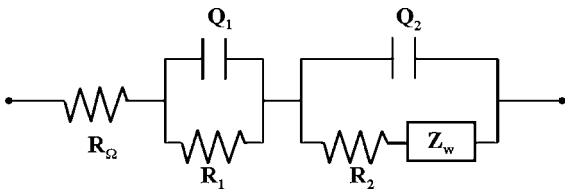

Fig. 5. The electrical equivalent circuit used to model impedance spectra of Figure 4.

high-frequency semicircle arises from the passive film on the electrodes, especially on the cathode [12–14]. On the other hand, our work performed on a single particle $LiCoO_2$ cathode [16] and a single particle MCMB anode [17] showed that the impedance spectrum of the $LiCoO_2$ cathode contained only one semicircle, whereas these of the MCMB anode exhibited at least two well-resolved semicircles. Dollé et al. [18] using a reference electrode inserted in a Li-ion cell identified that the charge-transfer process at the positive electrode is the limiting step during cycling or storage, whereas the capacity loss can be mostly attributed to the negative electrode and, more precisely, to the instability of its passivating layer. Yet, the three-electrode EIS measurement, is not straightforward, and reliable data and meaningful results depend on the shape, position, and configuration (optimization) of the reference electrode. A critical treatment of this problem was recently described by Adler [19].

From the foregoing, it is clear that the pair of semicircles observed in the impedance spectrum of the lithium-ion cell may not be easily resolved for the purpose of assigning to individual electrodes. Therefore, we will ascribe the high-frequency semicircle to the anode/electrolyte interface, and the low frequency semicircle to the cathode/electrolyte interface, and the diffusional impedance to solid-state diffusion of Li-ion in the bulk electrodes.

For evaluating impedance parameters of the lithium-ion battery at different SOCs, we employed the equivalent circuit shown in Figure 5. This circuit is basically similar to that used by Rodrigues et al. [12], Li et al. [13] and Suresh et al. [14], except for the diffusional impedance that did not appear in their impedance spectra. This is because their experiments were carried out at room temperature [12, 13] or limited to 40 °C [14].

In Figure 5, the element R_Ω represents the ohmic resistance of the cell, which includes electrolyte resistance and other resistances such as electrode bulk resistance, separator resistance, etc. The two capacitive semicircles are depressed; hence a constant phase element (CPE) denoted Q was considered. Q_1 taken in parallel to R_1 corresponds to the high frequency semicircle. R_2 and Q_2, are related to the low frequency semicircle. The CPE arises due to distribution of microscopic material properties and is suitable for electrodes that are made of fine particles of active materials and are thus neither as smooth or uniform as those in the lithium-ion battery. The admittance representation of $Q(\sec^n/\Omega)$ is given by [5]

$$Q = Q_0(j\omega)^n \tag{1}$$

where Q_0 is an adjustable parameter, $\omega=2\pi f$ is the radial frequency, and n is a number between -1 and 1. The CPE represents a resistor, R, when $n=0$, a capacitor, C, when $n=1$, and inductor, L, when $n=-1$ and a Warburg impedance when $n=0.5$. The impedance parameters obtained via CNLLS-fit analysis are listed in Tables 1–4. Parameters of the diffusion-related part of the Nyquist spectrum were omitted in the fitting procedure; an accurate fit was problematical as the lowest frequency used, 100 mHz, was not low enough.

As mentioned above, the ohmic resistance includes contributions from the electrolyte, separator, electrode materials, current collectors, and cell terminals. The electrolyte offers ionic resistance and the rest of the components electronic resistance. It is thus expected that the ionic conductivity of the electrolyte increases with increasing temperature if this parameter is due to electrolyte resistance alone. However, the data of Tables 1–4 show that, irrespective of the SOC, R_Ω is almost invariant up to 100 °C, whereas it increased at higher temperatures, which indicates changes in the ionic conductivity of the electrolyte. Electronic resistance increase of conductors with temperature is most probably negligible in this temperature range.

Also observed in Tables 1–4, R_1 decreased when either the SOC or the temperature increased. For charged cells, the high frequency semicircle was no longer seen at temperatures higher than 100–110 °C and even fitting the spectra considering $R_1||Q_1$ did not improve the

Table 1. Impedance parameters of the Li-ion polymer cell at SOC = 0%

Parameter	Temperature/°C							
	25	50	75	100	110	120	125	130
R_Ω/Ω	0.047	0.047	0.042	0.045	0.052	0.060	0.064	0.069
R_1/Ω	0.054	0.021	0.008	0.005	0.010	0.013	0.013	0.013
Q_1	0.424	1.082	0.534	0.070	0.034	0.025	0.154	0.126
n_1	0.550	0.550	0.750	1.000	0.988	0.982	0.947	0.985
R_2/Ω	0.260	0.046	0.012	0.005	0.007	0.008	0.016	0.022
Q_2	2.947	2.638	1.900	0.943	0.512	0.259	0.019	0.019
n_2	0.910	1.000	0.990	1.000	1.000	1.000	1.000	0.976

Table 2. Impedance parameters of the Li-ion polymer cell at SOC = 25%

Parameter	Temperature/°C							
	25	50	75	100	110	120	125	130
R_Ω/Ω	0.052	0.046	0.046	0.046	0.047	0.052	0.056	0.061
R_1/Ω	0.046	0.026	0.006	0.002	0.0014	No	No	No
Q_1	0.311	2.45	0.826	0.314	0.283	No	No	No
n_1	0.58	0.45	0.78	1.000	1.000	No	No	No
R_2/Ω	0.197	0.036	0.011	0.006	0.005	0.006	0.005	0.004
Q_2	2.867	2.570	1.629	0.956	0.663	0.988	1.230	1.066
n_2	0.872	0.999	1.000	1.000	1.000	0.843	0.840	0.860

NO – not observed.

Table 3. Impedance parameters of the Li-ion polymer cell at SOC = 75%

Parameter	Temperature/°C							
	25	50	75	100	110	120	125	130
R_Ω/Ω	0.048	0.045	0.043	0.045	0.055	0.067	0.073	0.086
R_1/Ω	0.042	0.014	0.003	0.001	NO	NO	NO	NO
Q_1	0.198	1.621	0.409	0.94	NO	NO	NO	NO
n_1	0.660	0.620	1.000	1.000	NO	NO	NO	NO
R_2/Ω	0.142	0.018	0.007	0.004	0.006	0.005	0.003	0.003
Q_2	3.056	2.340	1.189	0.867	0.395	0.257	0.297	0.254
n_2	0.818	1.000	1.000	1.000	0.966	1.000	1.000	1.000

NO – not observed.

Table 4. Impedance parameters of the Li-ion polymer cell at SOC = 100%

Parameter	Temperature/°C							
	25	50	75	100	110	120	125	130
R_Ω/Ω	0.054	0.051	0.050	0.053	0.056	0.067	CV	
R_1/Ω	0.030	0.016	0.003	0.001	no	no		
Q_1	0.306	1.629	0.43	0.71	no	no		
n_1	0.644	0.640	1.000	1.000	no	no		
R_2/Ω	0.119	0.023	0.008	0.006	0.006	0.006		
Q_2	3.305	2.304	1.151	0.650	0.525	0.698		
n_2	0.800	1.000	1.000	1.000	0.984	0.905		

NO – not observed; CV – cell vented.

fitting. There is also a dependence of R_2 on both SOC and temperature: (i) for charged cells, R_2 decreased with increasing temperature up to 100 °C and was more or less stable for higher temperatures. (ii) For uncharged cells, R_2 decreased up to 100 °C and increased for higher temperatures. This increase in R_2 happens together with the increase in R_Ω observed in Table 1. Figure 6 shows pictures of the cells after impedance experiments reported in Figure 4. Swelling of the cells was strongly dependent on the SOC, i.e., the expansion increased as the SOC increased.

3.3. *Evaluation of kinetic parameters of the polymer Li-ion cell reaction*

Suresh et al. [14] have analyzed impedance data related to Li-ion cells using the Butler–Volmer equation for activation-controlled charge-transfer reactions, and evaluated the kinetic parameters such as the transfer coefficient α and the activation energy E_a, of the cell according to the following equation:

$$\ln(R_{ct}/T) = \ln k + (E_a/RT) - \alpha \ln \mathrm{SOC} \tag{2}$$

where k is a constant, which is independent of SOC and temperature. On differentiation of Equation 2, one obtains:

$$\frac{\mathrm{d}\ln(R_{ct}/T)}{\mathrm{d}(1/T)} = \frac{E_a}{R} \tag{3}$$

$$\frac{\mathrm{d}\ln(R_{ct}/T)}{\mathrm{d}\ln \mathrm{SOC}} = -\alpha \tag{4}$$

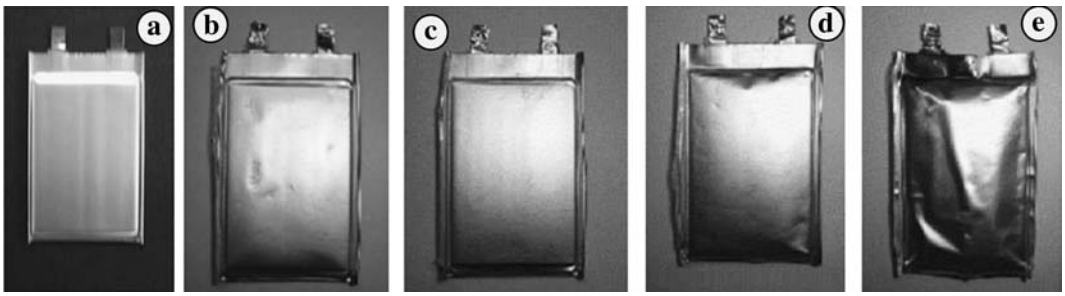

Fig. 6. Pictures of various polymer Li-ion batteries: (a) fresh cell, and after impedance experiments showed in Figure 4 for cells charged to (b) 0%, (c) 25%, (d) 75%, (e) and 100% SOC.

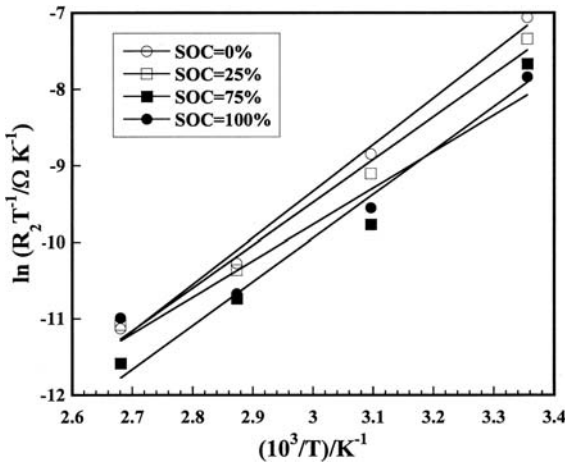

Fig. 7. Plot of $\ln(R_2/T)$ against inverse of temperature (T) for several SOCs (indicated on the figure).

The variations of $\ln(R_2/T)$ with 10^3/T up to 100 °C, and $\ln(R_2/T)$ with ln SOC are shown in Figures 7 and 8, respectively. The values of E_a obtained from Figure 7 for different SOC values are in the range 0.4–0.6 eV: these values are similar to those reported for a non-polymer Li-ion cells but for a temperature variation limited to 40 °C [14]. The α values obtained from Figure 8 are in the range 0.35–0.45 for $25 < T < 110$ °C, which is close to 0.5, a value expected for a reversible electrochemical reaction. However, for temperatures greater than 110 °C, α reached 0.087, indicating a high irreversible electrochemical reaction. We have to emphasize that for $T > 75$ °C, the plots exhibit a minimum at 75% SOC. Exactly, why is not known. Thus, it is apparent from the above discussion that the low frequency semicircle in the impedance spectra (Figure 4) arises from the charge-transfer processes of the Li-ion cell.

A similar analysis was applied to the high frequency semicircle in order to examine if this semicircle was also due to electron transfer. A plot of $\ln(R_1/T)$ versus ln SOC was linear (Figure 9) and a linear fit of the data resulted in a value of α increasing from 0.30 to 0.53 as the temperature increased from 25 to 100 °C. Additionally a plot of $\mathrm{d}\ln(R_1/T)/\mathrm{d}(1/T)$ yielded values of E_a in the range 0.36–0.53 eV (Figure 10). These observations also indicate that the high frequency semicircle corresponds to an electron transfer reaction. The reversibility is improved with increasing temperature and the charge transfer process became very fast, which explains the non-appearance of the high frequency semicircle for temperatures greater than 100 °C. Additionally, if R_1 were due to a surface film at the cathode, one would expect a higher value of R_1 in the fully charged state, since at this voltage a slight electrolyte decomposition at the surface of the highly oxidizing positive potentials

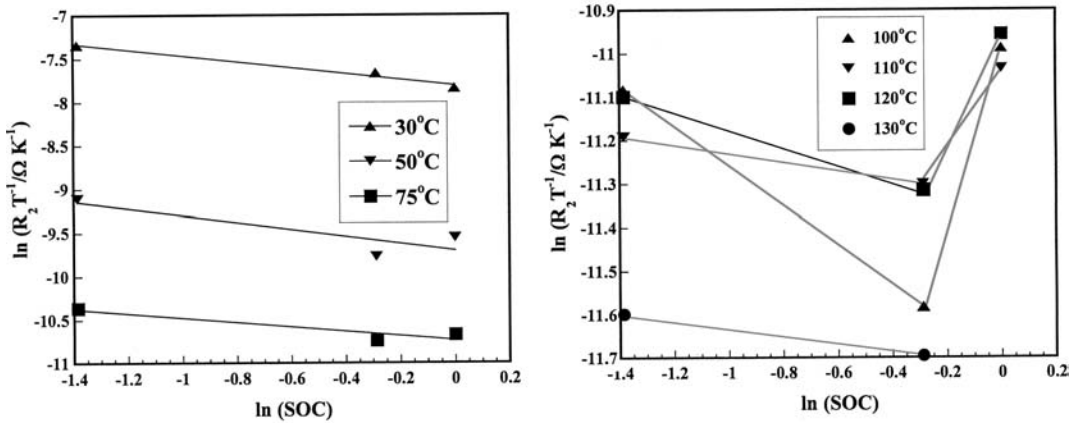

Fig. 8. Plot of $\ln(R_2/T)$ against SOC at various temperatures (indicated on the figure).

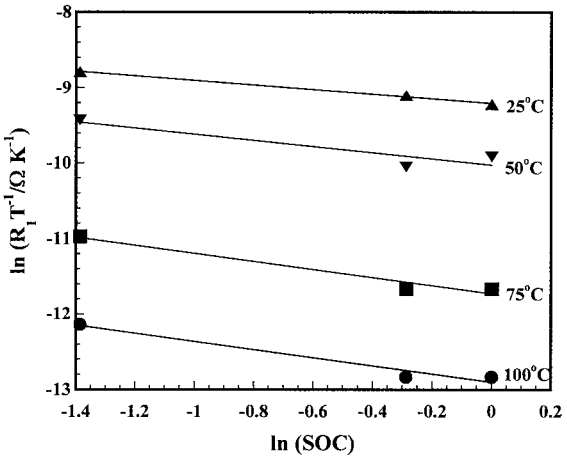

Fig. 9. Plot of $\ln(R_1/T)$ against SOC at various temperatures (indicated on the figure).

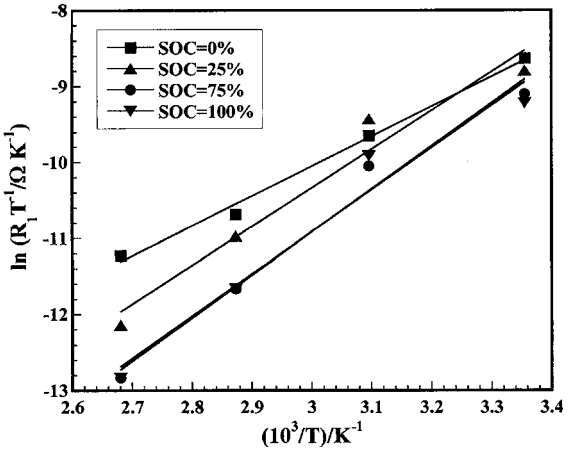

Fig. 10. Plot of $\ln(R_1/T)$ against inverse of temperature (T) for several SOCs (indicated on the figure).

results in the formation of a surface film. This is not the case here, where for a given temperature R_1 is generally higher in contrast to fully lithiated cathodes (Tables 1–4).

3.4. *Effect of aging on the impedance parameters*

The cells were subjected to thermal ageing for one week at SOC=0% and 100% at 30 and 100 °C, respectively. Figure 11 covers a one-week variation of R_Ω, R_1, R_2, and the cell voltage. There are several interesting features:

(i) There is no significant variation of the resistance parameters upon storage time for fully charged cells. We notice, however, a slight increase in R_1 and R_2 for fully discharged cells after 5 days of storage.
(ii) Upon storage the cell voltage dropped in a similar way for both cells. However, the magnitude in the drop was smaller for a charged cell (by ca. 0.04 V) than for an uncharged cell (by ca. 1 V). Even with this difference, the drop rate increase starts after 5 days of storage for both cells.

The resistance of a surface passive layer on the electrodes, R, i.e., a resistance for the lithium-ion migration through the surface layer and C its capacitance, are commonly described in the literature by Equations 5 and 6 [20]

$$R = \rho l/A \tag{5}$$

$$C = \varepsilon A/l \tag{6}$$

where l is the thickness of the surface layer, ε and ρ, respectively, its resistivity and its permittivity, and A is the electrode surface area. A decrease (thinning of the layer)/increase (thickening of the layer) in R will be accompanied by an increase/decrease in C if we assume that the surface is not too much affected by the intercalation process. Thus the non-variations of R_1 and R_2 observed in Figure 11 are not in agreement with predictions of Equations 5 and 6 for a surface layer process. Even the slight increase in R_1 and R_2 noticed for uncharged cells can not be explained as due to surface layers because we observed that Q_1 and Q_2 increased in disaccord with Equation 6 (assimilating Q to C).

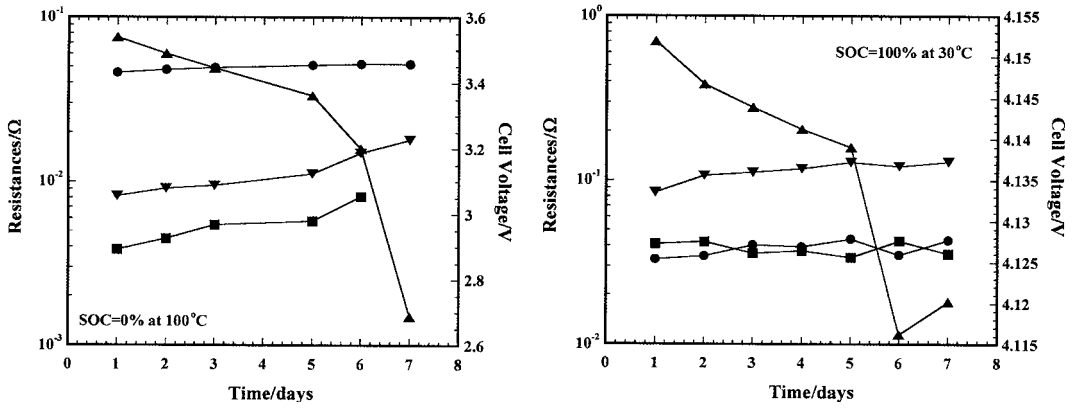

Fig. 11. Variation of R_Ω, R_1, R_2 and cell voltage upon storage of two polymer Li-ion polymer batteries for one week under experimental conditions reported in the figure. (●) R_Ω, (■) R_1, (▼) R_2, and (▲) OCV.

The drop for uncharged cells simply describes an end of complete discharge of the negative electrode, which still contains some lithium after discharge down to cut off (0% SOC). On the other hand, the voltage decrease during storage at 30 °C of 100% SOC reflects the self-discharge of the positive electrode (voltage depends on SOC) from reduction by electrolyte.

From the above analysis of Sections 3.3 and 3.4, neither R_1 nor R_2 can be explained on the basis of surface film formation alone but rather to processes occurring at the anode/electrolyte and cathode/electrolyte interfaces.

3.5. *Factors responsible for the rise in the cell impedance at high temperatures*

In all cases R_2 is always higher than R_1 upon storage, upon charging, or upon changing the temperature (at least up to 110 °C). According to the three-electrode EIS measurements [18], we can assign the low frequency semicircle to process occurring at the cathode/electrolyte interface and the high frequency to these happening at the anode/electrolyte interface, which is also in agreement with the interpretation of Nagasubramanian et al. [21].

Due to the change in film composition of the electrode during the experiment the charge-transfer resistance changes value. It is likely that the SEI formed on the anode is damaged upon increase in temperature, which will cause the dissolution of the film into the electrolyte. The degradation of the SEI at each electrode is different. Progressive destruction of the layer will make charge-transfer faster (Li-ions do not have to migrate first through a resisting layer) with a higher extent at the anode and explains why the high frequency semicircle is no longer seen at temperatures higher than 100 °C. At these stages, the diffusion process starts to be dominant as observed in Figure 4.

Du Pasquier et al. used a differential scanning calorimetry (DSC) and showed that the thermal decomposition of the SEI layer in the presence of a solvent starts at temperatures as low as 110 °C [22]. At around 100 °C, the metastable components of the SEI at the anode decompose very rapidly. This provides a small temperature boost to the remaining reactants in the cell as proposed by Dahn et al. [23]. More recently, Doughty et al. [24], have shown, with DSC measurements, that thermal reactions below 100 °C begin for the anode, followed by higher temperature reactions in the cathode. This exactly coincides with the first trigger temperature observed in thermal-cut off profile of the cell (Figure 3). Thus when the layer components go into the electrolyte, it can be expected that the electrolyte resistance will increase. The values of R_Ω are appreciably higher than the values of R_1 and R_2 for temperatures exceeding 50 °C. Thus it can be assumed that change in electrolyte composition is the main factor responsible for the rise in the cell impedance at high temperatures as demonstrated in Figure 12.

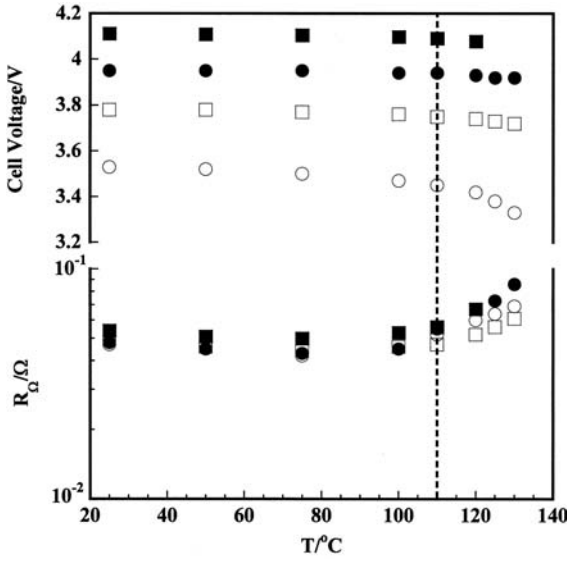

Fig. 12. Variation of the cell voltage and ohmic resistance (R_Ω) when the cells were heated from ambient to 130 °C.

4. Conclusions

Irrespective of the state of charge, all cells exhibited shutdown characteristics at around 133 °C, accompanied by a rise in the internal impedance (at 1 kHz) and at a few degrees higher by a fluctuation in the open-circuit-voltage at zero. A post-mortem observation of the cells revealed swelling and rupture of the cells due to the evolution of non-condensable gases at higher temperature.

Analysis of ac impedance behavior of the PLBs in the temperature range 25–110 °C for various SOC values showed that the high frequency semicircle is due to surface film and electrode reactions occurring at the anode/electrolyte, whereas the low frequency semicircle to surface film and electrode reactions occurring at the cathode/electrolyte interface. By means of the Butler-Volmer equation, the transfer coefficient, and activation energy of the cell for both anode and cathode reactions were evaluated.

Although there is no evidence from experiments that limited electrolyte decomposition has a strong influence on ionic conductivity, we assume that the main factor responsible for the rise in cell impedance at high temperatures is the change in electrolyte composition induced by the dissolution of the SEI components formed at the anode. Production of small a quantity of gas due to this decomposition within the electrode pores or in the separator could be a possible explanation.

References

1. J.-S. Hong, H. Maleki, S. Al Hallaj, L. Redey and J.R. Selman, *J. Electrochem. Soc.* **145** (1998) 1489.
2. S. Al Hallaj, H. Maleki, J.S. Hong and J.R. Selman, *J. Power Sources* **83** (1999) 1.

3. J.R. Selman, S. Al Hallaj, I. Uchida and Y. Hirano, *J. Power Sources* **97–98** (2001) 726.
4. G. Venugopal, *J. Power Sources* **101** (2001) 231.
5. B.A. Boukamp, *Equivalent Circuit User's Manual*, University of Twente (1989).
6. F.C. Laman, M.A. Gee and J. Denovan, *J. Electrochem. Soc.* **140** (1993) L51.
7. A.J. Bradley and R.E. White, *J. Power Sources* **70** (1998) 48.
8. G. Venugopal, J. Moore, J. Howard and S. Pendalwar, *J. Power Sources* **77** (1999) 34.
9. X. Liu, H. Kusawake and S. Kuwajima, *J. Power Sources* **97–98** (2001) 661.
10. F. Huet, *J. Power Sources* **70** (1998) 59.
11. K. Ozawa, *Solid State Ionics* **69** (1994) 212.
12. S. Rodrigues, N. Munichandraiah and A.K. Shukla, *J. Solid State Electrochem.* **3** (1999) 397.
13. J. Li, E. Murphy, J. Winnick and P.A. Kohl, *J. Power Sources* **102** (2001) 294.
14. P. Suresh, A.K. Shukla and N. Munichandraiah, *J. Appl. Electrochem.* **32** (2002) 267.
15. M.G.S.R. Thomas, P.G. Bruce and J.B. Goodenough, *J. Electrochem. Soc.* **132** (1985) 1521.
16. K. Dokko, M. Mohamedi, T. Itoh, M. Nishizawa, M. Umeda and I. Uchida, *J. Electrochem. Soc.* **148** (2001) A422.
17. M. Umeda, K. Dokko, Y. Fujita, M. Mohamedi, I. Uchida and J.R. Selman, *Electrochim. Acta* **47** (2001) 885.
18. M. Dollé, F. Orsini, A.S. Gozdz and J.-M. Tarascon, *J. Electrochem. Soc.* **148** (2001) A851.
19. S.B. Adler, *J. Electrochem. Soc.* **1149** (2002) E166.
20. E. Peled, *in* J.P. Gabano (Ed), *Lithium Batteries* (Academic Press, London, 1983), p. 60.
21. G. Nagasubramanian, R.G. Jungst and D.H. Doughty, *J. Power Sources* **83** (1999) 193.
22. A. Du Pasquier, F. Disma, T. Bowmer, A.S. Gozdz and G. Amatucci and J.-M. Tarascon, *J. Electrochem. Soc.* **145** (1998) 472.
23. T.D. Hatchard, D.D. MacNeil, A. Basu and J.R. Dahn, *J. Electrochem. Soc.* **148** (2001) A755.
24. D.H. Doughty, P.C. Butler, R.G. Jungst and E.P. Roth, *J. Power Sources* **110** (2002) 357.